Japanese Journal of Applied Physics

Real-Time Imaging of Vortex–Antivortex Annihilation in $Bi_2Sr_2CaCu_2O_{8+\delta}$ Single Crystals by Low Temperature Scanning Hall Probe Microscopy

To cite this article: Munir Dede *et al* 2006 *Jpn. J. Appl. Phys.* **45** 2246

Japanese Journal of Applied Physics
Vol. 45, No. 3B, 2006, pp. 2246–2250

Real-Time Imaging of Vortex–Antivortex Annihilation in $Bi_2Sr_2CaCu_2O_{8+\delta}$ Single Crystals by Low Temperature Scanning Hall Probe Microscopy

Munir DEDE, Ahmet ORAL, T. YAMAMOTO[1], Kazuo KADOWAKI[1] and Hadas SHTRIKMAN[2]

Department of Physics, Bilkent University, 06800 Ankara, Turkey
[1]*Institute of Materials Science, University of Tsukuba, 1-1-1 Tennodai, Tsukuba, Ibaraki 305-8573, Japan*
[2]*Weizmann Institute of Science, Department of Condensed Matter Physics, IL-76100 Rehovot, Israel*

(Received July 4, 2005; accepted October 12, 2005; published online March 27, 2006)

Vortices in superconductors play an important role in operating limits and applications of the superconductors. Scanning Hall probe microscopes have proven themselves to be quantitative and non-invasive tools for investigating magnetic samples down to 50 nm scale. Penetration of vortices in high quality single crystal $Bi_2Sr_2CaCu_2O_{8+\delta}$ superconductor has been studied in real-time with single vortex resolution at 77 K using a low temperature scanning Hall probe microscope (LT-SHPM). Vortices have been observed to be annihilated by the antivortices in small M–H loops. [DOI: 10.1143/JJAP.45.2246]

KEYWORDS: BSCCO, superconductivity, vortices, Hall effect, scanning Hall probe microscopy

1. Introduction

Scanning Hall probe microscopy (SHPM)[1,2] is a quantitative and non-invasive technique for imaging localized surface magnetic field distribution on sample surfaces with high spatial and magnetic field resolution of ~50 nm and $100\,\mathrm{mG}/\sqrt{\mathrm{Hz}}$, over a wide range of temperatures, 30 mK–300 K. This new technique offers great advantages and complements the other magnetic imaging methods like magnetic force microscopy (MFM),[3] magnetic near field scanning optical microscopy (MNSOM)[4] and Kerr microscopy.[5] MFM invasive and non quantitative, MNSOM is difficult to operate, Kerr technique has low resolution. The SHPM technique is non invasive and gives quantitative data. Moreover, the Hall sensor's used in the SHPMs do not saturate under high external fields and the technique has been shown to operate up to 7 T.[6] The microscope can also be used as a local scanning magnetometer with extremely high magnetic moment sensitivity and can measure magnetization loops of very small magnetic nanostructures. In SHPM, a micro-Hall probe is scanned over the sample surface to measure the perpendicular component of the surface magnetic fields using conventional scanning tunneling microscopy (STM) positioning techniques as shown in Fig. 1. The SHPM has started as an obscure scanning probe microscopy (SPM) method with very limited performance and applications at cryogenic temperatures, to a well-developed magnetic characterization technique with 50 nm spatial resolution[7] and extremely high field resolution. The first microscope[1] could get an image over many hours at 4.2 K due to noise; in contrast to 1 frame/s scan speeds of modern SHPMs operating at room temperature. The performance of the SHPMs can be improved further down to 10–20 nm spatial resolution, 6–8 frames/s scan speeds limited by the electronics,[8] without sacrificing the field resolution drastically. Unlike Squids or MFM, where sensitivity decreases with the areal size or the volume of the sensor, sensitivity in Hall sensors decreases linearly with the width of the hall sensor. Therefore, decreasing the Hall sensor size from 50 to 10–20 nm, will decrease the sensitivity by a factor of 5–2.5. Magnetic field penetrates into superconductors in the form of vortices carrying single flux quantum, Φ_0. At the center of the vortex the sample is no more superconductive; moreover the motion of the vortices weakens the superconductivity. Imaging of the vortices in static and dynamic cases is of great importance without disturbing them. The vortex structure and dynamics of vortices give important data about the physical properties of the superconducting material. The pinning of these vortices and the strength of the pinning determines the J_C.[9] SHPMs are well suited for this application with unprecedented field resolutions over wide temperature range. In this work, we describe the real-time imaging of vortex–antivortex interactions using a low temperature scanning Hall probe microscope (LT-SHPM).

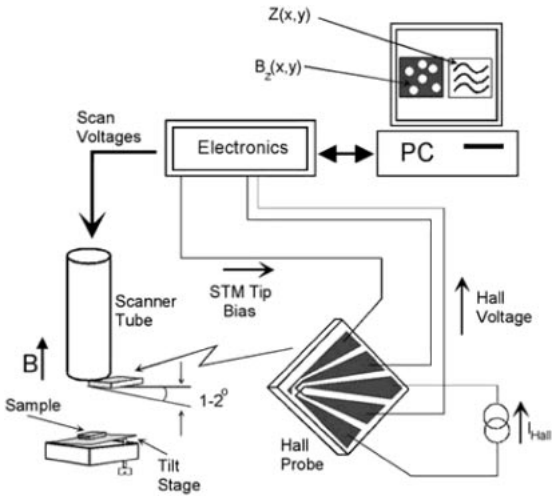

Fig. 1. Schematic diagram of LT-SHPM.

2. Experimental

2.1 Scanning Hall probe microscope

In SHPM, the Hall sensor is positioned close to a gold-coated corner of a deep etch mesa, which serves as STM tip as shown in Fig. 2. The Hall probe chip is tilted ~1° with respect to sample ensuring that the corner of the mesa is the highest point. The microscope can be run in two modes: STM tracking and lift-off mode. In the STM tracking mode, the tunnel current between the corner of the Hall sensor chip and the sample is measured and used to drive the feedback loop enabling the simultaneous measurement of both STM

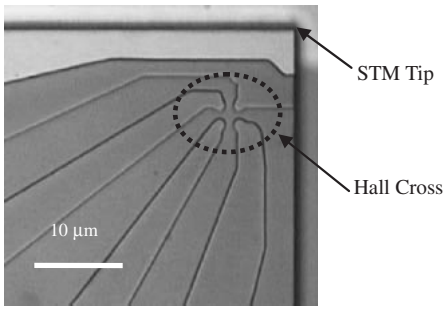

Fig. 2. Optical micrograph of a 1 μm GaAs/AlGaAs 2DEG thin film micro-Hall. Gold coated corner of the chip on the left of Hall cross serves as STM tip.

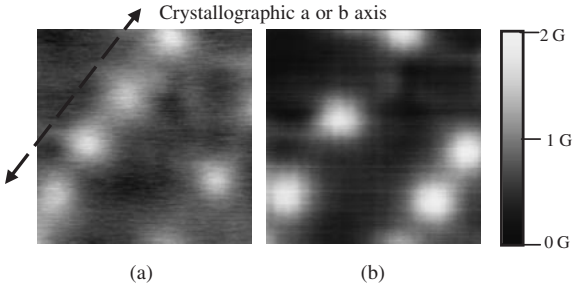

Fig. 3. Vortex images in BSCCO(2212) obtained by LT-SHPM. Images show $\sim 13 \times 13\,\mu m^2$ scan area. Chain like behavior of the vortices can clearly be seen at two different runs (a) and (b).

topography and the magnetic field distribution of the sample surface. This mode of operation gives the highest sensitivity because of the smallest probe-sample separation at all times, but with the drawback of being slow. In the lift-off mode, however, the Hall sensor is lifted off to a certain height above the sample and the head can be scanned extremely fast ($\sim$1 s/frame) for measurements of the local magnetic field distribution. Atomic force microscope (AFM) tracking SHPM has recently been developed, integrating a micro-Hall sensor onto a SiN AFM cantilever[10] and onto a GaAs AFM cantilever with sharp tip.[11] The force is measured and controlled by optical[10] or piezoresistive[11] detection.

The LT-SHPM[12] used in this study is very compact (23.6 mm OD) commercial microscope and can be operated between 30 mK–300 K and tested up to 9 T external fields. The sample can also be positioned within 3 mm in *XY* directions.

In SHPM the minimum detectable magnetic field is limited mainly by the noise of the Hall sensor. Hall sensors are driven with a DC current (I_{HALL}) and the Hall voltage measured using a low noise amplifier positioned close to the nano-Hall probe. The amplifier's gain and bandwidth are adjustable parameters. The minimum detectable magnetic field with a Hall probe can be written as,[2]

$$B_{min} = V_{noise}/(R_H I_{HALL}) \quad (1)$$

where V_{noise} is the total voltage noise at the input of the Hall amplifier. The voltage noise of the amplifier can usually be made negligible. The V_{noise} has two components; Johnson noise due to the series resistance of the Hall sensor (R_s) and the $1/f$ noise. It is desirable to drive the Hall probe with the highest permissible current. However, the voltage noise of series resistance R_s increases due to heating of the charge carriers and the lattice. Therefore, the Hall current cannot be increased indefinitely and there is a maximum useable $I_{HALLmax}$.

2.2 *Hall probe fabrication*

GaAs/GaAlAs two dimensional electron gas (2DEG) Hall probes are fabricated with optical lithography using standard clean room processing techniques.[13,14] Figure 2 shows a $\sim$1 μm size 2DEG micro-Hall probe with a Hall coefficient of $R_H \sim 0.16\,\Omega$/Gauss and a series resistance of $R_s = 5-6\,k\Omega$ at 77 K. At that temperature, GaAs/AlGaAs 2DEG micro-Hall sensors exhibit a noise level of $\sim 1\,mG/\sqrt{Hz}$.

3. Results

3.1 *Imaging of superconductors and magnetization measurements*

Magnetic field penetrates into superconductors as quantised fluxons, called Abrikosov vortices. We have investigated the flux penetration into high quality single crystal BSCCO(2212) with single flux quantum (vortex) resolution using a low temperature SHPM at 77 K.[15] The samples were prepared with traveling zone method[16,17] and had a $T_c \sim 87$ K, determined by a SQUID magnetometer.

The sample is glued on the sample holder from its corners using silver paint. Since BSCCO is a layered material, where the layers are weakly linked to each other, a scotch tape is used for cleaving the sample to obtain a clean and flat surface before loading into the microscope. The tape is carefully applied to the surface of the sample and then peeled off, removing with it a thin layer of material. The LT-SHPM and the cryostat system were degaussed at 110–130 K and zero field cooled to 77 K. SHPM images were obtained in the in lift-off mode where the active area of the probe is pulled back $\sim$650 nm from the sample. Figure 3 shows images of trapped vortices due to earth's magnetic field. It can be seen that the trapped flux lie in stripes parallel to one of the crystallographic axes (*a* or *b*) separated by regions free from strong pinning sites.[18]

We have also performed quasi-real time SHPM imaging to study how the vortices penetrate into the BSCCO superconductor. We first degaussed the system at 110 K and then applied field opposite to the earth's magnetic field during the cool down to 77 K. We adjusted the strength of the counter field such that we observe no vortices within the scan area at 77 K. Then, starting with the zero field, the magnitude of the external field is decreased to -4 Oe and flux penetration is observed in real-time, as the microscope is scanned across the surface with high speed, 1.8 s/frame.

The magnetic flux observed to be penetrating into the sample in the form of single flux quanta. Figure 4 shows some of the consecutive images showing penetration of antivortices. We acquired 100 images in lift-off mode while the probe is separated 650 nm from the sample and converted these into a movie.[19] We observed that the vortices prefer to penetrate into the crystal along the *a* or *b* crystallographic directions. The anti-vortices seem to stop at the pinning sites momentarily as they move under the effect of the external field.

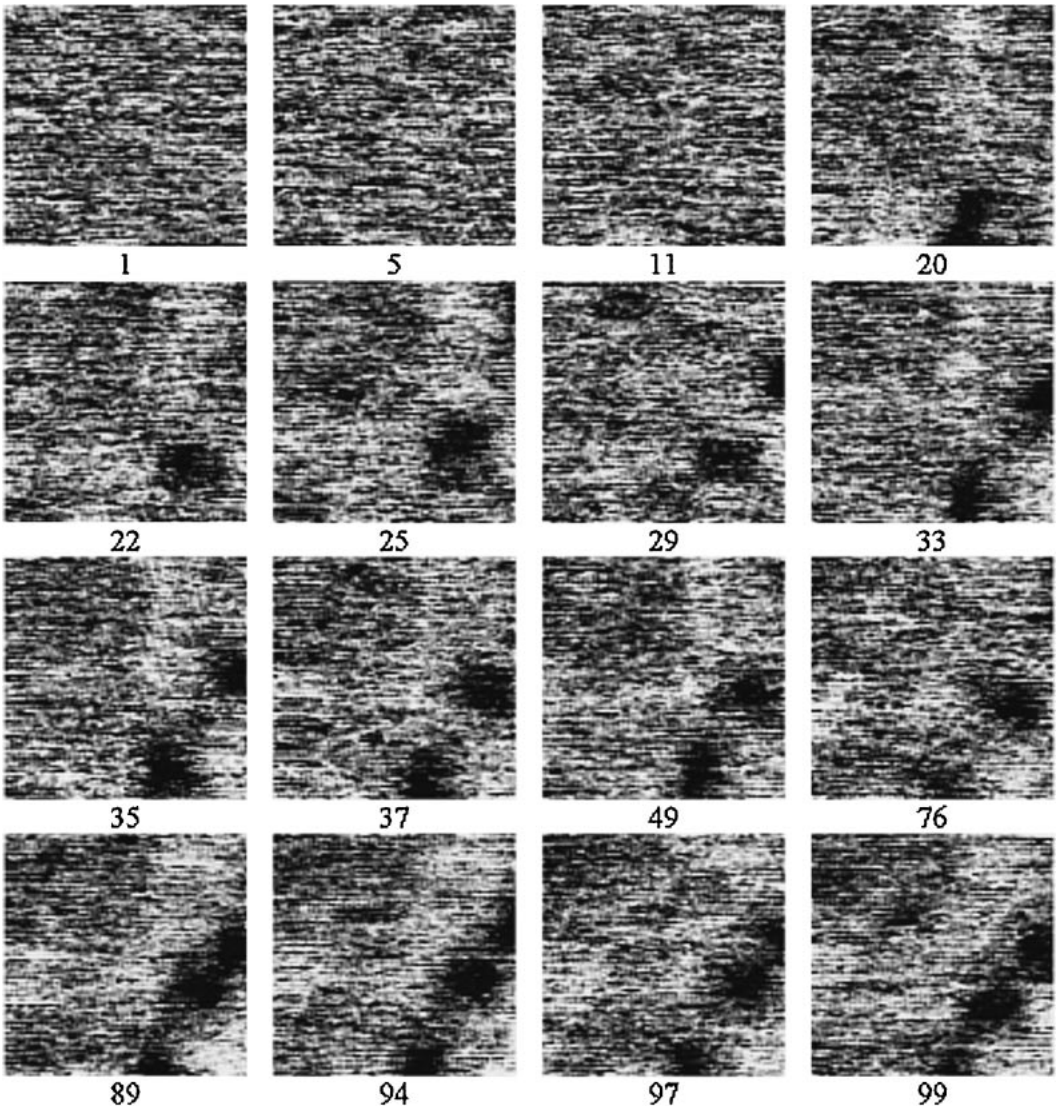

Fig. 4. Snapshots of the antivortex penetration movie. Numbers show the individual frame numbers out of 100 images.[19)]

In another run, we repeated the same procedure to obtain a virgin (vortex free) state and performed a complete *B–H* curve to a maximum field of +6 Oe and a minimum field of of −6 Oe as we scanned the microscope in real-time. We captured 1000 SHPM images in lift-off mode while the probe is separated 650 nm from the sample. The images were then processed into another movie.[20)] The snapshots of the movie are given in Fig. 5. The vortices are observed to be penetrating into the BSCCO single crystal in the positive field ramp along the crystallographic directions *a* or *b*. They start to leave the crystal along the same direction as the external field is decreased back to zero. However, they can not completely be swept away. As the external field is ramped towards the negative values, the anti-vortices seem to be penetrating into the crystal, annihilating the vortices first and establishing themselves in the sample.

SHPMs can also be used to perform local magnetization measurements, over an area defined by the Hall probe size. The Hall sensors are probably the smallest magnetometers that can be constructed with extremely high magnetic moment sensitivity.

Static local magnetization measurements were also performed at 77 K on the BSCCO(2212) sample. Figure 6 shows the *M–H* curve obtained with the SHPM with a maximum applied field of ±138 Oe. Jumps in the local magnetic induction curve around ±100 Oe are due to vortex lattice melting transitions.

4. Discussion and Conclusions

We have observed the penetration of vortices and vortex–antivortex annihilation in BSCCO single crystals at 77 K in real-time using SHPM. The vortices are observed to be penetrating into the crystal along one of the crystallographic directions, *a* or *b*. This indicates that there are strong pinning sites running along one of the crystallographic directons, observed in all samples grown in different batches. These pining sites can be due to concentration fluctuations or crystallographic defects in the material. Perhaps the local T_c varies across the material along these pinning sites. Moreover, as magnetic flux penetrates into the material in the form of Abrikosov vortices, they seem to prefer the paths along the pinning sites. Identification of the cause of these sites may help to increase the crystal quality or J_{max} of the material and hence can increase the potential of the BSCCO in industrial applications.

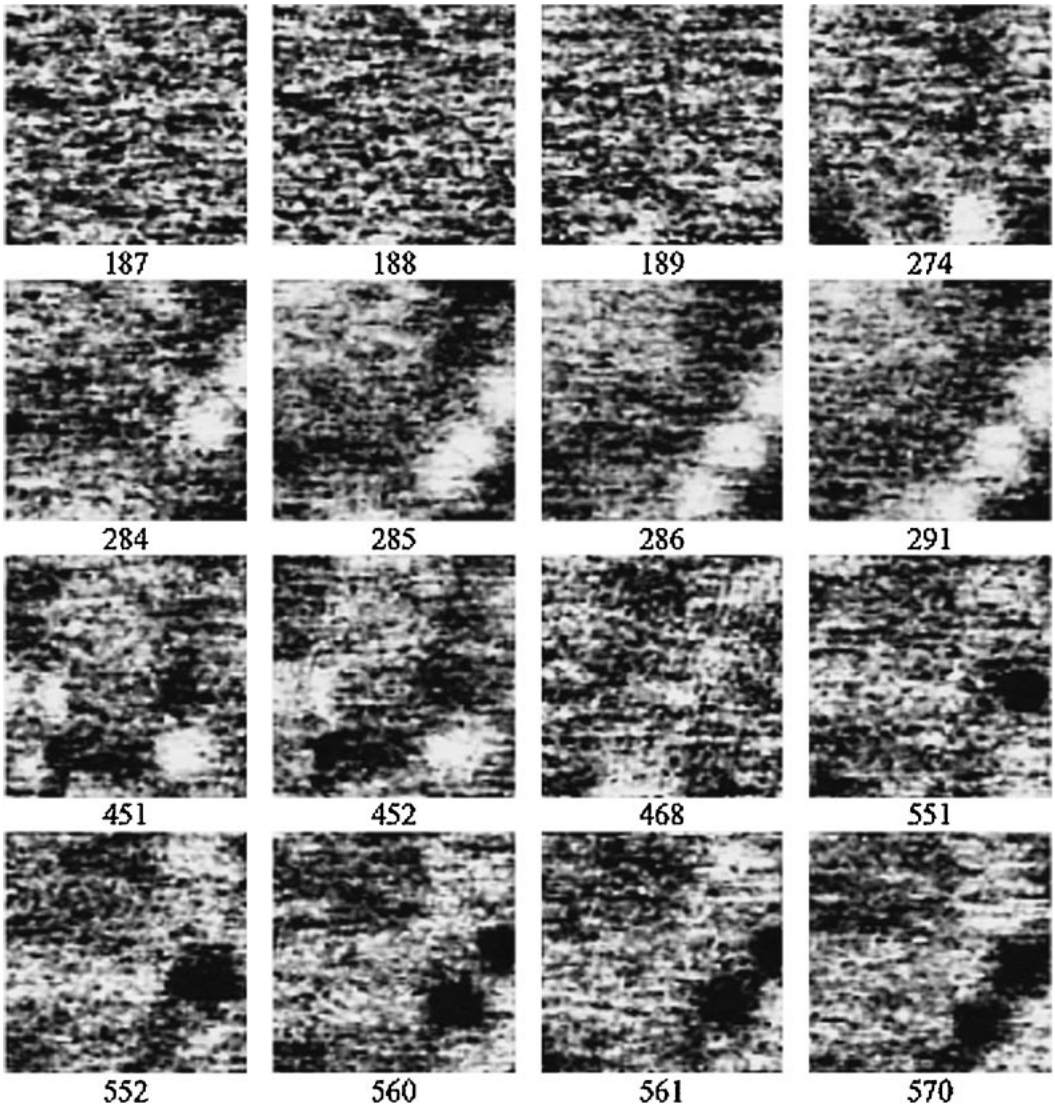

Fig. 5. Snapshots from the vortex–antivortex annihilation movie obtained during a ±6 Oe *B–H* curve. Numbers show the individual frame numbers out of 1000 images.[20)]

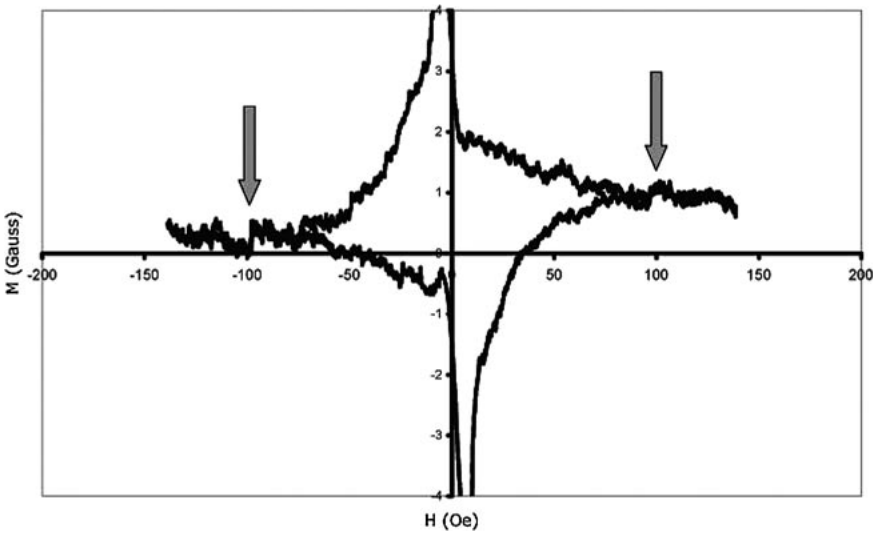

Fig. 6. *M–H* curve showing the vortex lattice melting transition at 77 K.

Acknowledgements

This project has been supported by TÜBİTAK Project No: TBAG-1878, NanoMagnetics Instruments Ltd. and The Turkish Academy of Sciences, TÜBA in Turkey. This work has also been supported by the 21st Century COE (Center of

Excellence) Program, "Promotion of Creative Interdisciplinary Materials Science for Novel Functions", from the Ministry of Education, Culture, Sports, Science and Technology (MEXT), Japan.

1) A. M. Chang, H. D. Hallen, L. Harriot, H. F. Hess, H. L. Loa, J. Kao, R. E. Miller and T. Y. Chang: Appl. Phys. Lett. **61** (1992) 1974.
2) A. Oral, S. J. Bending and M. Henini: Appl. Phys. Lett. **69** (1996) 1324.
3) Y. Martin and H. K. Wickramasinghe: Appl. Phys. Lett. **50** (1987) 1455.
4) E. Betzig, J. K. Trautman, R. Wolfe, E. M. Gyorgy, P. L. Finn, M. H. Kryder and C. H. Chang: Appl. Phys. Lett. **61** (1992) 142.
5) F. Schmidt and A. Hubert: J. Magn. Magn. Mater. **61** (1986) 307.
6) M. Dede and A. Oral: unpublished.
7) A. Sandhu, K. Krosawa, M. Dede and A. Oral: Jpn. J. Appl. Phys. **43** (2004) 777.
8) M. J. Rost: Rev. Sci. Instrum. **76** (2005) 053710.
9) A. K. Ghosh and A. N. Basu: Physica C **361** (2001) 135.
10) B. K. Chong, H. Zhou, G. Mills, L. Donaldson and J. M. R. Weaver: J. Vac. Sci. Technol. A **19** (2001) 1769.
11) A. J. Brook, S. J. Bending, J. Pinto, A. Oral, D. Ritchie, H. Beere, A. Springthorpe and M. Henini: J. Micromech. Microeng. **13** (2003) 124.
12) Low Temperature Scanning Hall Probe Microscope (LT-SHPM), NanoMagnetics Instruments Ltd., 17 Croft Road, Oxford, U.K. (www.nanomagnetics-inst.com)
13) A. Oral, S. J. Bending and M. Henini: J. Vac. Sci. Technol. B **14** (1996) 1202.
14) A. Sandhu, H. Masuda, A. Oral and S. J. Bending: Jpn. J. Appl. Phys. **40** (2001) L524.
15) A. Oral, J. C. Barnard, S. J. Bending, I. I. Kaya, S. Ooi, H. Taoka, T. Tamegai and M. Henini: Phys. Rev. Lett. **80** (1998) 3610.
16) K. Kadowaki and T. Mochiku: Proc. Int. Natl. Workshop on Superconductivity, Honolulu, Hawaii, U.S.A., June 23–26, 1992 p. 112.
17) T. Mochiku and K. Kadowaki: Physica C **235–240** (1994) 523.
18) A. Oral, J. C. Barnard, S. J. Bending, S. Ooi, H. Taoka, T. Tamegai and M. Heini: Phys. Rev. B **56** (1997) R14295.
19) Movie can be seen and downloaded from http://www.fen.bilkent.edu.tr/~spm/video/vortex1.avi
20) Movie can be seen and downloaded from http://www.fen.bilkent.edu.tr/~spm/video/vortex2.avi